Journal of the American College of Cardiology Vol. 59, No. 2, 2012

Published by Elsevier Inc.
ISSN 0735-1097/$36.00
doi:10.1016/j.jacc.2011.09.045

Deformation Dynamics and Mechanical Properties of the Aortic Annulus by 4-Dimensional Computed Tomography

Insights Into the Functional Anatomy of the Aortic Valve Complex and Implications for Transcatheter Aortic Valve Therapy

Ashraf Hamdan, MD,*† Victor Guetta, MD,* Eli Konen, MD,† Orly Goitein, MD,† Amit Segev, MD,* Ehud Raanani, MD,‡ Dan Spiegelstein, MD,‡ Ilan Hay, MD,* Elio Di Segni, MD,*† Michael Eldar, MD,* Ehud Schwammenthal, MD, PHD*

Tel Hashomer, Israel

Objectives The purpose of this study was to assess deformation dynamics and in vivo mechanical properties of the aortic annulus throughout the cardiac cycle.

Background Understanding dynamic aspects of functional aortic valve anatomy is important for beating-heart transcatheter aortic valve implantation.

Methods Thirty-five patients with aortic stenosis and 11 normal subjects underwent 256-slice computed tomography. The aortic annulus plane was reconstructed in 10% increments over the cardiac cycle. For each phase, minimum diameter, ellipticity index, cross-sectional area (CSA), and perimeter (Perim) were measured. In a subset of 10 patients, Young's elastic module was calculated from the stress-strain relationship of the annulus.

Results In both subjects with normal and with calcified aortic valves, minimum diameter increased in systole (12.3 ± 7.3% and 9.8 ± 3.4%, respectively; $p < 0.001$), and ellipticity index decreased (12.7 ± 8.8% and 10.3 ± 2.7%, respectively; $p < 0.001$). The CSA increased by 11.2 ± 5.4% and 6.2 ± 4.8%, respectively ($p < 0.001$). Perim increase was negligible in patients with calcified valves (0.56 ± 0.85%; $p < 0.001$) and small even in normal subjects (2.2 ± 2.2%; $p = 0.01$). Accordingly, relative percentage differences between maximum and minimum values were significantly smallest for Perim compared with all other parameters. Young's modulus was calculated as 22.6 ± 9.2 MPa in patients and 13.8 ± 6.4 MPa in normal subjects.

Conclusions The aortic annulus, generally elliptic, assumes a more round shape in systole, thus increasing CSA without substantial change in perimeter. Perimeter changes are negligible in patients with calcified valves, because tissue properties allow very little expansion. Aortic annulus perimeter appears therefore ideally suited for accurate sizing in transcatheter aortic valve implantation. (J Am Coll Cardiol 2012;59:119–27) © 2012 by the American College of Cardiology Foundation

The challenges of transcatheter valve therapy have forced structural heart specialists to rediscover the complex anatomy of the aortic valve in all its intricate details (1,2). Although much was known for centuries (3), insight into the in vivo anatomy of the aortic valve complex—unavailable from surgical or pathological inspection of a non-beating heart—became possible only with modern 3-dimensional imaging techniques (4–10). Importantly, sizing for transcatheter aortic valve implantation (TAVI), unlike with surgical valve replacement, relies exclusively on cardiac imaging. Accurate assessment of the target anatomy, specifically the aortic annulus—its size, shape, and mechanical properties—is paramount to avoid complications such

See page 128

From the *Heart Center, Chaim Sheba Medical Center, Tel Hashomer, Sackler Faculty of Medicine, Tel-Aviv University, Tel Hashomer, Israel; †Department of Radiology, Sheba Medical Center, Tel Hashomer, Sackler Faculty of Medicine, Tel-Aviv University, Hashomer, Israel; and the ‡Department of Cardiac Surgery, Chaim Sheba Medical Center, Tel Hashomer, Sackler Faculty of Medicine, Tel-Aviv University, Hashomer, Israel. Dr. Segev is a proctor for Edwards LifeSciences. Dr. Schwammenthal is a paid consultant for Medtronic Ventor Technologies, LTD, Netanya, Israel. All other authors have reported that they have no relationships relevant to the contents of this paper to disclose. Drs. Hamdan and Guetta contributed equally to this work.

Manuscript received April 21, 2011; revised manuscript received September 12, 2011, accepted September 13, 2011.

Abbreviations and Acronyms

CT = computed tomography
CSA = cross-sectional area
ECG = electrocardiogram
EI = ellipticity index
LV = left ventricular
Max = maximum diameter
Min = minimum diameter
Perim = perimeter
TAVI = transcatheter aortic valve implantation

as device dislodgment, perivalvular leakage, or annular rupture (10,11). In case of beating heart procedures like TAVI, assessing the dynamic aspects of functional anatomy, such as potential time-varying changes of the aortic annulus throughout the cardiac cycle, may be particularly important.

The purpose of the present study was therefore to investigate deformation dynamics and in vivo mechanical properties of the aortic annulus in patients with and without calcified aortic valves and to analyze the implications for the clinical practice of TAVI. Specifically, the major hypotheses of the study were as follows: 1) cyclic conformational changes of the anatomic structures that form the annulus will generate periodic variations in the degree of its ellipticity and thus its cross-sectional area and diameters; 2) mechanical properties of the annulus allow only minimal stretch under physiological pressures (if any), particularly in patients with calcified valves; and 3) aortic annulus perimeter will therefore, by continuity, remain stable throughout the cardiac cycle, despite changes in shape and area, and thus represents the most robust parameter for accurate sizing in TAVI.

These hypotheses were tested in a cohort of candidates for TAVI who underwent 4-dimensional computed tomography and compared with findings in subjects without evidence of cardiac disease.

Methods

Study population. The study group included 35 consecutive patients with symptomatic severe aortic stenosis evaluated with computed tomography (CT) before TAVI and 11 subjects without evidence of cardiovascular disease, initially referred to CT angiography to rule out coronary artery disease, who served as a control group (Table 1). The study was approved by the local institutional review board.

Acquisition protocol. All patients underwent CT angiography for evaluation of aortic annulus, aorta, and the iliofemoral arteries before TAVI using a 256-slice system (Brilliance iCT, Philips Healthcare, Cleveland, Ohio). Data were acquired with a collimation of 96 × 0.625 mm and a gantry rotation time of 330 ms. The tube current was 485 mA at 100 kV, the pitch value was 0.2, and the scan direction was cranio-caudal.

Intravenous injection of 60 to 90 ml of nonionic contrast agent (Iomeron 350, Bracco, Milan, Italy) at a flow rate of 5 ml/s was followed by a 30-ml saline chase bolus (5 ml/s). Automated peak enhancement detection in the descending aorta was used for timing of the scan. Data acquisition was automatically initiated at a threshold level of 100 Hounsfield units. Acquisition was performed during an inspiratory breath-hold while the electrocardiogram (ECG) was recorded simultaneously to allow retrospective gating of the data. For assessment of the aortic annulus, the 3-dimensional dataset of the contrast-enhanced scan was reconstructed at 10% increments over the cardiac cycle, generating a 4-dimensional CT dataset. All images were reconstructed with a slice thickness of 0.67 mm and a slice increment of 0.34 mm.

Subjects in the control group were scanned (according to the clinical indication) from the carina to below the diaphragmatic face of the heart. Because of the increased susceptibility of younger subjects to ionizing radiation, ECG-gated tube current modulation was used to minimize radiation exposure.

Assessment of the aortic annulus. The complete dataset was transmitted to a dedicated CT workstation (Philips, Extended Brilliance Workspace, version 4.5) to allow for multiplanar reformations. The aortic annulus was defined as the virtual circumferential connection of the aortic leaflets' basal attachments (virtual basal ring) (1,2). Accordingly, the standard coronal and sagittal views were used for initial orientation and definition of the lowest point of attachment of the aortic leaflets (11) to generate double-oblique axial images of the aortic annulus, as shown in Figure 1. The following measurements were performed at each 10% phase of the cardiac cycle (Fig. 1): Minimum diameter of the aortic annulus (Min), maximum diameter (Max), cross-sectional area (CSA), and perimeter (Perim). Ellipticity index (EI) was calculated as the ratio of Max to Min. In order to minimize measurement error, the aortic annulus plane was reconstructed in 1 phase, and the same multiplane reformations were used for measurements throughout all other phases (with slight adjustments to account for motion of the left ventricle during long-axis contraction, as necessary).

Calculation of Young's elastic modulus. In a subgroup of 10 patients, left ventricular (LV) pressure tracings before TAVI were analyzed by dividing them into 10 equal intervals between 2 consecutive R waves on the ECG. LV pressures and perimeters at corresponding phases of the cardiac cycle were related to derive the Young elastic modulus. Because invasive pressure measurements and CT could not be performed simultaneously, only patients whose heart rate differed <10 beats/min between CT examination and invasive pressure measurements, and whose systolic

Table 1 Baseline Characteristics of Study Population

	Patients With Aortic Stenosis	Normal Subjects
Age, yrs	80.1 ± 7.4	56.2 ± 11.8
Male	16 (46)	5 (11)
BMI, kg/m^2	28.1 ± 4.7	29.1 ± 8.0
BSA, m^2	1.86 ± 0.25	1.87 ± 0.22
CAD	12 (34)	0 (0)
Previous MI	7 (20)	0 (0)
Previous CAGB	6 (17)	0 (0)

Values are mean ± SD or n (%).
BMI = body mass index; BSA = body surface area; CABG = coronary artery bypass grafting; CAD = coronary artery disease; MI = myocardial infarction.

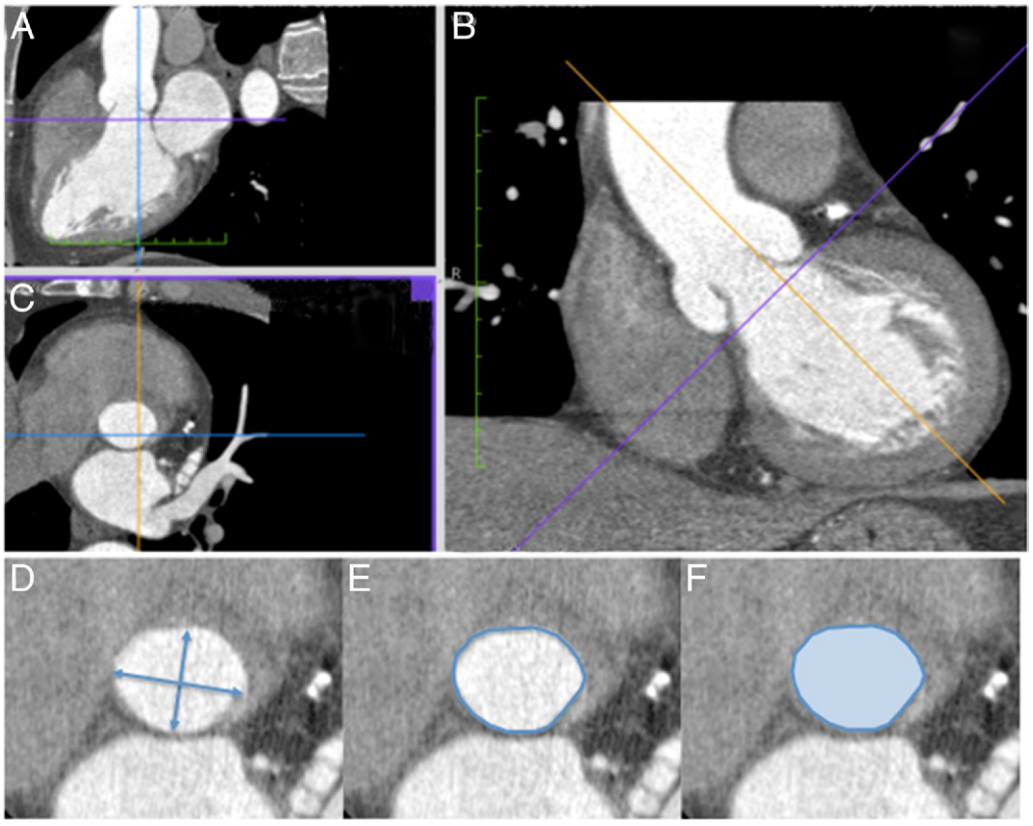

Figure 1 **Reconstruction of the Aortic Annulus by Computed Tomography**

Reconstruction of the aortic annulus from the sagittal **(A)** and the coronal planes **(B)** using double oblique multiplane reformations. The aortic annulus is defined as the circumferential connection of the aortic leaflets' most basal attachments in the reconstructed axial plane **(C)**. Measurements of the minimum and maximum diameter **(D)**, the perimeter **(E)**, and the area **(F)** were performed in this plane.

aortic blood pressure differed <15 mm Hg, were included in this analysis. The Young module is defined as the slope of the tensile stress-strain curve in its initial linear portion (12):

$$E = \frac{\sigma}{\varepsilon} = \frac{F/A}{\Delta L/L_0}$$

where E is the Young modulus, σ is the tensile stress, ε is the tensile strain, F is the force applied through the cross-sectional area A, and ΔL/Lo is the length change of an object as a fraction of its original length. For a 3-dimensional annular elastic element such as the aortic annulus (Fig. 2), F is given by the distending force that results from the LV pressure acting on its endocardial surface area Ae. Substituting P × Ae for F yields:

$$\sigma = \text{LV pressure} \frac{Ae}{A}$$

Because Ae = 2πr × h and A = h × b, their common dimension h cancels out:

$$\sigma = \text{LV pressure} \frac{2\pi r}{b} \text{ or } \sigma = \text{LV pressure} \times \text{perimeter/b}$$

For an annular structure, tensile strain is given by the fractional change of the perimeter:

$$\varepsilon = \Delta\text{perimeter}/\text{perimeter}_0$$

When applied to the aortic annulus, E, the slope of the tensile stress-strain curve, can therefore be determined as:

$$E = \frac{\sigma}{\varepsilon} = \frac{\text{LV pressure} \times \text{perimeter/b}}{\Delta\text{perimeter}/\text{perimeter}_0}$$

LV pressure, perimeter, and fractional perimeter change were measured at each of the 10 phases. For annulus thickness b, the thickness of the aorto-mitral continuity measured at 70% of the cardiac cycle was used. Because E is the ratio of stress, which has units of pressure, to strain, which is dimensionless, E has units of pressure (MPa or GPa).

In normal subjects, in whom an invasively measured LV pressure curve was not available, the slope of the stress-

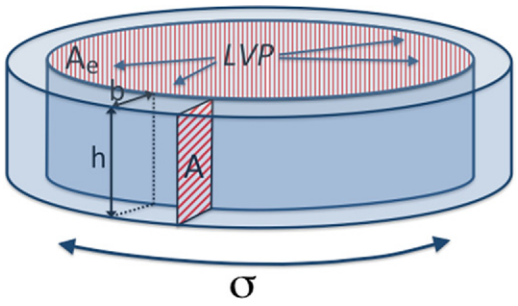

Figure 2 **Aortic Annulus Modeled as an Annular Elastic Element**

Schematic of the aortic annulus modeled as an annular elastic element with the height h, the thickness b, and the cross-sectional area A. Left ventricular pressure (LVP) acting on the endocardial surface Ae generates the distending force across A, which is the tensile stress σ.

strain relationship was determined from 2 points, at peak systole (using the noninvasively determined systolic aortic pressure at the time of the examination) and mid-diastole (assuming a normal diastolic ventricular pressure of 10 mm Hg; all normal subjects had a normal echocardiographic study, including a normal transmitral flow profile and normal diastolic tissue Doppler velocity curves).

Statistical analysis. Continuous variables are expressed as mean ± SD, and results are presented in box plot format where appropriate. In order to account for the potential confounding effect of variations in body size, measurements of diameter, area, and perimeter were indexed for body surface area. Differences between systolic and diastolic values of parameters, as well as between the relative changes of these parameters, were tested using Student paired *t* test with Bonferroni correction for multiple comparisons. The elastic modulus *E* was determined using linear regression analysis, and the correlation coefficient *r* and its square (r^2) were calculated for each regression. Differences in *E* between patients with aortic stenosis and subjects with normal aortic valves were tested using the Mann-Whitney *U* test. Interobserver variability was tested in 10 randomly selected study subjects according to the Bland and Altman method and included new multiplane reconstructions. In addition, intraclass correlation coefficient was determined.

Results

Figure 3 and Table 2 detail the observed changes of annular size and shape throughout the cardiac cycle: In both subjects with normal and with calcified aortic valves, there was a significant and substantial systolic increase in Min (12.3 ± 7.3% and 9.8 ± 3.4%, respectively; $p < 0.001$), with a significant and substantial decrease in ellipticity (12.7 ± 8.8%, $p = 0.002$; and 10.3 ± 2.7%, $p < 0.001$, respectively). Accordingly, CSA increased by 11.2 ± 5.4% and 6.2 ± 4.8%, respectively ($p < 0.001$). Although the systolic increase in perimeter also reached statistical significance ($p = 0.01$) due to consistent behavior, this change (2.2 ± 2.2%, and 0.56 ± 0.85%, respectively) was quantitatively unimportant and close to the range of inter-observer variability for individual measurements.

Figure 4 shows that the relative percentage difference between maximal and minimal values was indeed smallest for Perim when compared with Min, EI, and CSA, in both normal subjects ($p < 0.001$, 0.019, and < 0.001, respectively, after Bonferroni correction) as well as patients with aortic stenosis ($p < 0.001$ for all parameters after Bonferroni correction).

The Young module, calculated from the slope of the pressure/perimeter change relationship of 10 patients with calcified aortic valves, was calculated as 22.6 ± 9.2 MPa, and in normal subjects it was estimated as 13.8 ± 6.4 MPa (Fig. 5). Correlation coefficients *r* ranged from 0.52 to 0.93 (r^2 ranged from 0.27 to 0.87).

Interobserver variability and 95% limits (in parenthesis with identical units) were as follows: For Min, 0.06 ± 0.45 mm (−0.84, 0.96); for EI, 0.01 ± 0.05 (−0.09, 0.11); for

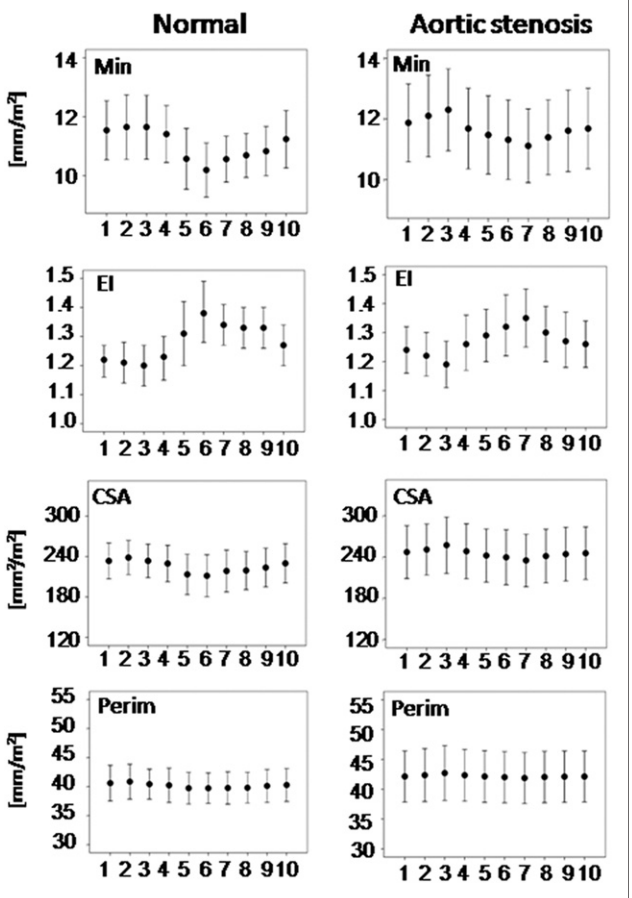

Figure 3 **Variation of Annular Dimensions Throughout the Cardiac Cycle**

Variation of annular dimensions throughout the cardiac cycle in normal subjects **(left)** and patients with calcified aortic stenosis **(right)**. From **top to bottom:** minimum diameter (Min), ellipticity index (EI), aortic annulus cross-sectional area (CSA), and perimeter (Perim).

Table 2 Maximum and Minimum Values of Aortic Annulus Dimensions in Normal Subjects and Patients With Severe Aortic Stenosis

Parameters	Normal Subjects			Patients With Aortic Stenosis			p Value	
	Max Values	Min Values	Delta %	Max Values	Min Values	Delta %	Max vs. Max*	Min vs. Min†
Min diameter index, mm/m^2 (absolute value in mm)	11.7 ± 1.1 (21.7 ± 1.8)	10.2 ± 0.9‡ (19.0 ± 2.6)	12.3 ± 7.3	12.3 ± 1.4 (22.6 ± 2.9)	11.1 ± 1.2‡ (20.4 ± 2.7)	9.8 ± 3.4	0.19	0.04
Ellipticity	1.38 ± 0.10	1.21 ± 0.07§	12.7 ± 8.8	1.35 ± 0.10	1.19 ± 0.08‡	10.3 ± 2.7	0.59	0.34
Area index, mm^2/m^2 (absolute value in mm^2)	239 ± 25 (448 ± 81.8)	211 ± 31‡ (398.7 ± 93.7)	11.2 ± 5.4	257 ± 40.9 (480.9 ± 108)	234 ± 38.2‡ (438.8 ± 103)	6.2 ± 4.8	0.14	0.07
Perimeter index, mm/m^2 (absolute value in mm)	40.9 ± 3.0 (76.1 ± 6.7)	39.7 ± 2.6‖ (74.1 ± 7.6)	2.2 ± 2.2	42.7 ± 4.6 (78.9 ± 8.7)	41.9 ± 4.3‡ (77.3 ± 8.6)	0.56 ± 0.85	0.17	0.11

Values are mean ± SD. *Max values in normal subjects versus Max values in patients with aortic stenosis; †Min values in normal subjects versus Min values in patients with aortic stenosis; ‡p < 0.001; §p = 0.002; ‖p = 0.01 for Max versus Min values in the same group by paired *t* test.
Max = maximum; Min = minimum.

CSA, 2.1 ± 12.2 mm^2 (−22.3, 26.5), and for Perim, 0.19 ± 0.41 mm (−0.63, 1.01). Intra-class correlation coefficient was 0.98 for Min, 0.90 for EI, and 0.99 for CSA and Perim.

Discussion

The present study demonstrates a predictable time variance of aortic annulus size throughout the cardiac cycle. Aortic annulus area increases from diastole to systole despite the fact that its circumference remains virtually constant in patients with calcified aortic valves and even in normal subjects increases only slightly. The increase in area is therefore almost exclusively the consequence of annular reshaping, not stretch: The ellipticity of the annulus decreases significantly from diastole to systole because of a significant increase in its anteroposteriorly oriented minor diameter, whereas its mediolaterally oriented diameter remains fairly constant.

Functional anatomy of the aortic annulus: valvular interdependence. The underlying mechanism of this dynamic aortic annular deformation can be understood from the functional anatomy of the left heart (Fig. 6). While the right ventricle has a dedicated outflow tract (the infundibulum), which is anatomically separated from its inflow by the crista supraventricularis, the LV chamber has essentially 1 common aorto-mitral orifice at its base (1,2,13,14). Consequently, the LV outflow, including the aortic annulus at its end, is not a dedicated anatomical structure, but rather marked out by surrounding boundaries. The structures forming or supporting the aortic annulus, defined as the virtual circumferential connection of the basal attachments of the aortic leaflets (1,2), consist mostly of fibrous tissue. This tissue extends posteriorly from the left fibrous trigone, the aorto-mitral continuity, and the right fibrous trigone into the membranous ventricular septum (anteriorly and to the right); only the left anterior aspect of the annulus is supported by myocardial fibers (1,2). Motion of fibrous tissue is necessarily dictated by a passive response to changes in pressure differences: in case of the aorto-mitral continuity, pressure differences between left ventricle and left atrium, and in case of the membranous septum, between the left and right ventricle.

In systole, the increase in LV pressure above the level of right ventricular and left atrial pressure will therefore act to shift the membranous septum and the aorto-mitral continuity apart, thus increasing the anteroposterior diameter of the annulus, which will become less elliptical (Fig. 6). The increase in the minor axis diameter seemed to be predominantly due to the motion of the aorto-mitral continuity, as described experimentally using radiopaque markers (13,14). In diastole, the LV pressure drop to levels below the left atrial pressure (mitral opening) will act to reverse the shift of the aorto-mitral continuity, decreasing the minor diameter of the annulus, which will become more elliptical (Fig. 6). These findings are in agreement with the recent in vivo demonstration that the projected surface areas of normal

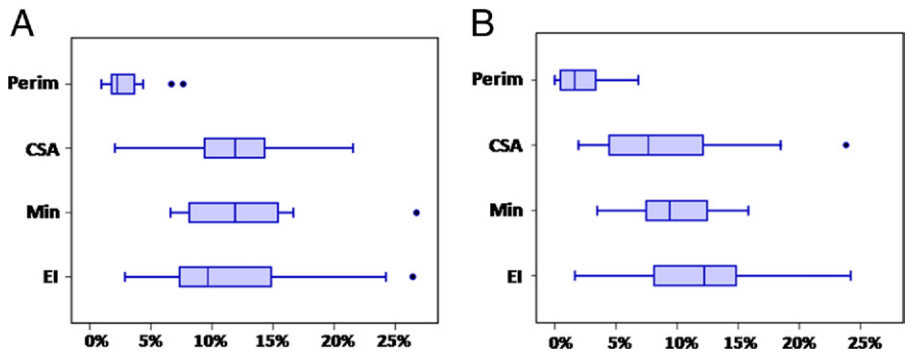

Figure 4 Relative Percent Change of Aortic Annulus Dimensions

Relative percentage difference between maximal and minimal values of aortic annulus measurements in normal subjects **(A)** and in patients with aortic stenosis **(B)**. **From top to bottom:** Perim, CSA, Min, and EI. Relative percentage changes were significantly smaller for Perim than for each of the other parameters. Abbreviations as in Figure 3.

aortic and mitral valves demonstrate coupled reciprocal behavior throughout the cardiac cycle (15).

The observed dynamics of aortic annular deformation during the cardiac cycle may confer important physiological advantages: Because the material properties of the structures that form the aortic annulus seem to allow only insignificant stretch under physiological pressures, a desirable increase in the cross-sectional outflow area during systolic ejection can only be achieved through conformational changes. Because for any given circumference a circular shape provides the greatest area, the aortic annulus can increase its CSA by assuming a more round shape through a posterior shift of the aorto-mitral continuity. Conversely, the diastolic anterior shift of the aorto-mitral continuity increases the ellipticity of the annulus and thus decreases its CSA. This, in turn, may act to reduce the wear force acting on the leaflet attachments of the closed aortic valve (because force equals pressure × area, the force acting on a closed aortic valve with a smaller area of attachment will be smaller for any given aorto-ventricular pressure difference).

The observed deformational dynamics of the aortic annulus essentially reflect a "valvular interdependence" of the aortic and mitral annulus, which are embedded within 1 common orifice, so that reciprocal changes of size and shape of each element result from the pressure-sensitive motion of its common aorto-mitral septum (aorto-mitral coupling).

Mechanical properties of the aortic annulus. Because the aortic annulus is not a histologically distinguishable structural entity, but rather a functional anatomic composite, it might be very difficult to determine its mechanical properties in vitro on a specimen. It seemed therefore most appropriate to assess the elastic modulus of the annulus in vivo using the very imaging technique used to define it. The Young elastic modulus was therefore determined from the relationship between invasive ventricular pressure measurements and time-corresponding CT measurements of the

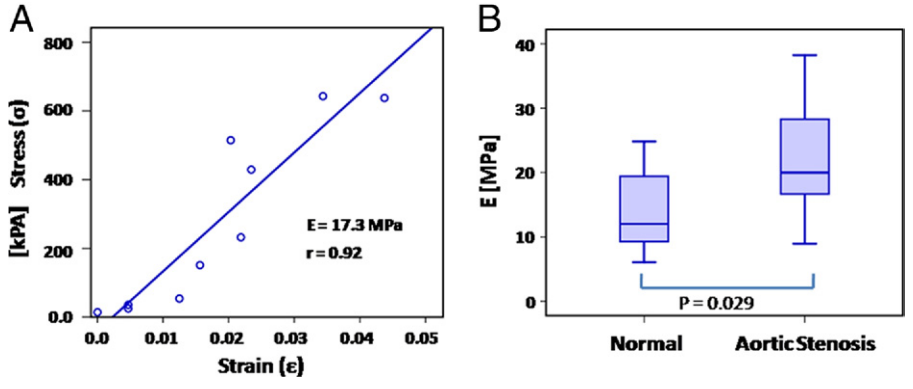

Figure 5 Stress-Stain Relationship and Elastic Modulus of the Aortic Annulus

(A) Representative example of the stress-strain relationship of the aortic annulus in a patient with calcified aortic stenosis. Stress (σ) is plotted on the y-axis, strain (ε) on the x-axis. The Young modulus E is determined as the slope of the regression function. **(B)** Box plot diagram of the Young modulus estimated in normal subjects and patients with aortic stenosis.

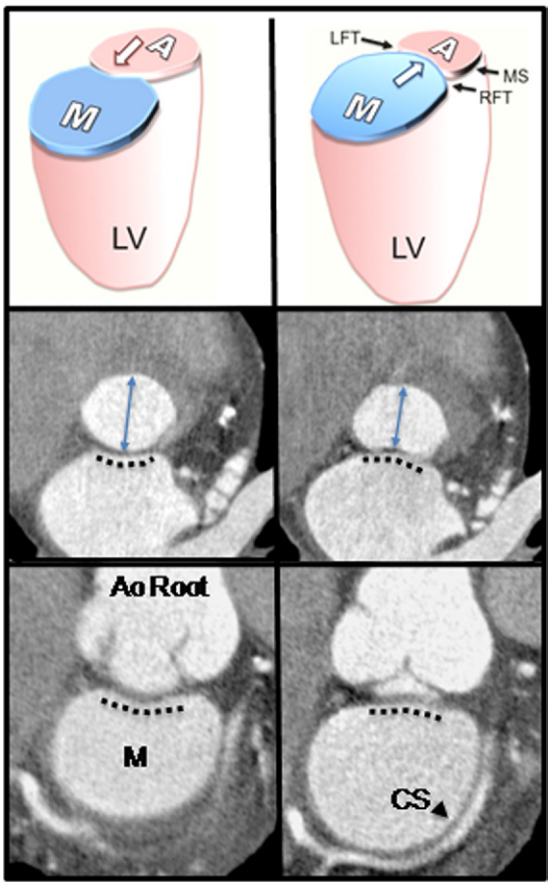

Figure 6 **Systolic and Diastolic Conformation of the Aorto-Mitral Orifice**

The **top panel** shows a schematic, the **middle panel** the aortic annulus plane, and the **bottom panel** the mitral annulus plane. In systole **(left)**, the aorto-mitral continuity is bending toward the mitral annulus. As a result, the aortic annulus anteroposterior diameter increases **(blue double arrows, middle panel)**, resulting in reduced ellipticity and a larger cross-sectional area. In diastole **(right)**, the aorto-mitral continuity is bending into the aortic annular plane. A = aortic annulus; Ao = aortic; CS = coronary sinus; LFT = left fibrous trigone; LV = left ventricle; M = mitral annulus; MS = membranous septum; RFT = right fibrous trigone.

annulus perimeter within the cardiac cycle. Although patients with calcified aortic valves showed a perimeter increase (strain) of only approximately 0.6% (maximally 1.8%) over a pressure range of 210 mm Hg, subjects with a normal aortic valve showed an increase of 2.2% (maximally 6.8%) over a lower pressure range (150 mm Hg). Consequently, the calculated Young module yielded an average value of approximately 23 MPa for patients with calcified aortic valves and 14 MPa for subjects with a normal aortic valve. These values are 60 times higher (patients with calcified valves) and 35 times higher (normal subjects) than those reported for soft tissues including muscle (0.3 to 0.4 MPa), while being significantly less than for 100% collagen fiber composites, load-bearing tendons (1 to 1.8 GPa), or cortical bones (15 to 20 GPa) (16–18).

The relatively high Young modulus indicates substantial material stiffness. This explains why the systolic perimeter increase (although consistently observed in the dataset and thus statistically significant) was very small in normal subjects and in patients with calcified aortic valves even in the range of the method's error for individual measurements. This is consistent with most CT studies, which have shown that neither circumference nor shape of the annulus change significantly after implantation of the Core Valve self-expandable transcatheter aortic valve (19). Even for the balloon-expandable Edwards Sapien transcatheter aortic valve, which is deployed with a pressure of 4 atm (3,040 mm Hg) and forces the annulus to assume a rounder shape, no significant increase in mean diameter was observed after implantation (no perimeter measurements are available from this study, mean diameter times π is an estimate of perimeter) (20). The current data may indicate that the annulus cannot be strained significantly without tear, further stressing the importance of accurate sizing.

Implications for the clinical practice of TAVI. Sizing consists of accurately fitting device dimensions to those of the target anatomy. The size of an aortic annulus with its generally elliptical shape cannot be accurately assessed by a 1-dimensional measurement such as a diameter. Variation in ellipticity was substantial in the patient population, and reliance on an anteroposterior diameter, typically estimated by standard echocardiography, may therefore be misleading, be-

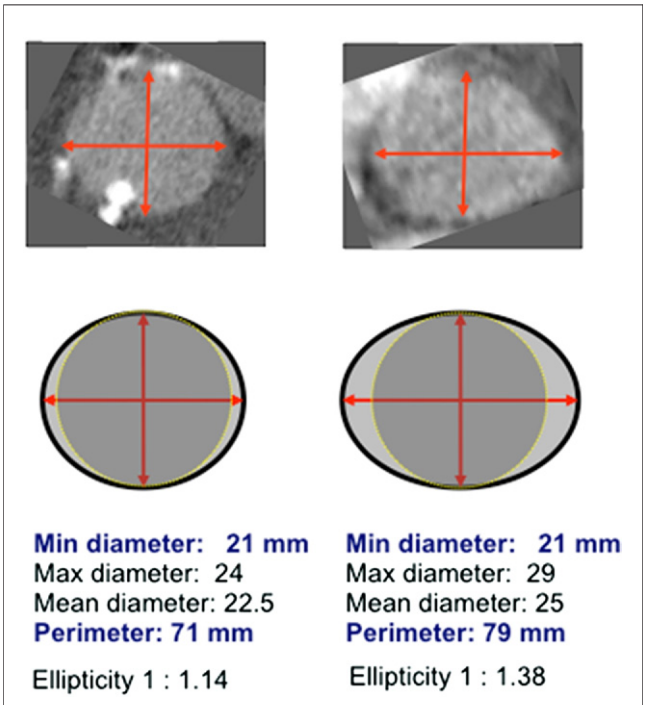

Figure 7 **Inter-Individual Differences in Aortic Annulus Ellipticity**

Comparatively round **(left)** and moderately elliptical **(right)** aortic annulus in 2 patients with aortic stenosis who have the same minimum diameter, but substantially different annular sizes, as indicated by an 8-mm difference in perimeter.

cause variations in ellipticity may result in striking differences in annular size for comparable anteroposterior diameters (Fig. 7).

The most suitable parameter of annulus size should ideally be one that integrates its dimensions across the whole 2-dimensional annular plane, is most stable throughout the cardiac cycle, and is independent of its shape. The present study demonstrates that aortic annulus perimeter fulfills all 3 conditions: 1) it circumferentially integrates annular diameters (mean circumferential diameter can be easily obtained by dividing perimeter into π); 2) it shows minimal variation during the cardiac cycle, because 3) it is not affected by shape changes (in contrast to area) and stretches only minimally under physiological pressures (relatively high Young modulus). The data therefore unequivocally support the use of perimeter-based sizing for TAVI, as also advocated by Piazza et al. (21) and Schultz et. al. (10,19).

Study limitations. The accuracy of estimating Young modulus may have been affected by nonsimultaneous measurements of LV pressures and perimeters (simultaneous measurements were neither feasible nor justifiable in this clinical setting). In order to minimize the potential impact of this effect, only data from patients who had comparable hemodynamics at both examinations were used.

Calculation of the Young elastic modulus implies the assumption that the strain observed is induced by the stress measured and thus reflects purely (passive) material properties. Although the anatomy of the aortic annulus is generally compatible with this assumption, several qualifiers are in place: 1) tethering forces of the contracting muscular septum on the membranous septum may render the latter less mobile than dictated by its intrinsic material properties; 2) tethering forces resulting from conformational changes of the ventricle and mitral annulus during the cardiac cycle as well as the aortic root could theoretically also affect annular motion; and 3) part of the aortic annulus (its left anterior aspect) is supported by actively contracting myocardial fibers. Consequently, the Young modulus calculated in this study using a lumped model approach should not be seen as a pure parameter of intrinsic material properties, but rather as a useful quantitative expression of the effective stress-strain relationship in vivo that is relevant to the clinical scenario.

Conclusions

Four-dimensional CT studies of the aortic valve complex demonstrate dynamical conformational changes throughout the cardiac cycle. The aortic annulus, generally elliptic, assumes a more round shape in systole, thus increasing cross-sectional flow area. In diastole, the increase in ellipticity results in a reduced area encompassed by the leaflets' basal attachments, reducing the force acting on the closed aortic valve. Despite these dynamic changes, aortic annulus perimeter variations are very small in normal subjects and essentially negligible in patients with calcified valves, presumably because tissue properties allow very little expansion. Aortic annulus perimeter appears therefore ideally suited for sizing in TAVI.

Acknowledgment

The authors thank Dr. Ilya Novikov for his expert statistical review and assistance.

Reprint requests and correspondence: Dr. Ashraf Hamdan, Heart Center, Chaim Sheba Medical Center, Tel Hashomer 52621, Israel. E-mail: Ashraf.Hamdan@sheba.health.gov.il.

REFERENCES

1. Piazza N, de Jaegere P, Schultz C, Becker AE, Serruys PW, Anderson RA. Anatomy of the aortic valvar complex and its implication for transcatheter implantation of the aortic valve. Circ Cardiovasc Interv 2008;174–81.
2. Anderson RH. The surgical anatomy of the aortic root. Multimed Man Cardiothorac Surg 2007. doi:10.1510/mmcts.2006.002527.
3. Leonardo da Vinci. Notes on the valves of the heart and flow of blood within it. The Royal Collection, © 2005, Her Majesty Queen Elizabeth II.
4. Doddamani S, Bello R, Friedman MA, et al. Demonstration of left ventricular outflow tract eccentricity by real time 3D echocardiography: implications for the determination of aortic valve area. Echocardiography 2007;24:860–6.
5. Doddamani S, Grushko M, Makaryus A, et al. Demonstration of left ventricular outflow tract eccentricity by 64-slice multi-detector CT. Int J Cardiovasc Imaging 2009;25:175–81.
6. Tops LF, Wood DA, Delgado V, et al. Noninvasive evaluation of the aortic root with multislice computed tomography. Implications for transcatheter aortic valve replacement. J Am Coll Cardiol Img 2008; 1:321–30.
7. Wood DA, Tops LF, Mayo JR, et al. Role of multislice computed tomography in transcatheter aortic valve replacement. Am J Cardiol 2009;103:1295–301.
8. Ng ACT, Delgado V, van der Kley F, et al. Comparison of aortic root dimensions and geometries before and after transcatheter aortic valve implantation by 2- and 3-dimensional transesophageal echocardiography and multislice computed tomography. Circ Cardiovasc Imaging 2010;3:94–102.
9. Messika-Zeitoun D, Serfaty JM, Brochet E, et al. Multimodal assessment of the aortic annulus diameter implications for transcatheter aortic valve implantation. J Am Coll Cardiol 2010;55:186–94.
10. Schultz CJ, Moelker A, Piazza N, et al. Three dimensional evaluation of the aortic annulus using multislice computer tomography: are manufacturer's guidelines for sizing for percutaneous aortic valve replacement helpful? Eur Heart J 2010;31:849–56.
11. Détaint D, Lepage L, Himbert D, et al. Determinants of significant paravalvular regurgitation after transcatheter aortic valve: implantation impact of device and annulus discongruence. J Am Coll Cardiol Intv 2009;2:821–7.
12. Bird J, Ross C. Mechanical Engineering Principles. Oxford, UK: Newnes, 2002.
13. Lansac E, Lim KH, Shomura Y, et al. Dynamic balance of the aortomitral junction. J Thorac Cardiovasc Surg 2002;123:911–8.
14. Glasson JR, Komeda MK, Daughters GT, et al. Three-dimensional regional dynamics of the normal mitral anulus during left ventricular ejection. J Thorac Cardiovasc Surg 1996;111:574–85.
15. Veronesi F, Corsi C, Sugeng L, et al. A study of functional anatomy of aortic-mitral valve coupling using 3D matrix transesophageal echocardiography. Circ Cardiovasc Imaging 2009;2:24–31.
16. Mow VC, Hayes WC, editors. Basic Orthopaedic Biomechanics. New York, NY: Raven Press, 1991.
17. An KN, Sun YL, Luo ZP. Flexibility of type I collagen and mechanical properties of connective tissue. Biorheology 2004;41:239–46.

18. Rho JY, Ashman RB, Turner CH. Young's modulus of trabecular and cortical bone material: ultrasonic and microtensile measurements. J Biomech 1993;26:111–9.
19. Schultz CJ, Weustink A, Piazza N, et al. Geometry and degree of apposition of the CoreValve Revalving System (CRS) with multislice computer tomography after implantation in patients with aortic stenosis. J Am Coll Cardiol 2009;54:911–8.
20. Blanke P, Siepe M, Reinöhl J, et al. Assessment of aortic annulus dimensions for Edwards SAPIEN Transapical Heart Valve implantation by computed tomography: calculating average diameter using a virtual ring method. Eur J Cardiothorac Surg 2010;38:750–8.
21. Piazza N, Lange R. Imaging of Valvular Heart Disease: I Can See Clearly Now. Anatomy of the aortic valve. 2010. Available at: http://org.crsti.dliv2010.s3.amazonaws.com/pdfs/034_Ovality_of_the_aortic_valve_annulus.pdf. Accessed April 15, 2011.

Key Words: aortic annulus ■ computed tomography ■ transcatheter aortic valve implantation.